NASA TECHNICAL MEMORANDUM

NASA TM X-62,453

NASA TM X- 62,453



# VIBRATION-TRANSLATION ENERGY TRANSFER IN ANHARMONIC DIATOMIC MOLECULES: II. THE VIBRATIONAL QUANTUM NUMBER DEPENDENCE

Robert L. McKenzie

Ames Research Center
Moffett Field, Calif.

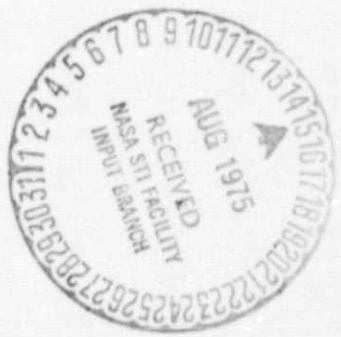


June 1975

| 1. Report No. | 2. Government Accession No. | 3. Recipient's Catalog No. |
|---|---|---|
| NASA TM X-62,453 | | |

| 4. Title and Subtitle | 5. Report Date |
|---|---|
| Vibration-Translation Energy Transfer in Anharmonic Diatomic Molecules: II. The Vibrational Quantum-Number Dependence | 6. Performing Organization Code |

| 7. Author(s) | 8. Performing Organization Report No. |
|---|---|
| Robert L. McKenzie | A-6152 |
| | 10. Work Unit No. 506-25-61-01-00-21 |

| 9. Performing Organization Name and Address | 11. Contract or Grant No. |
|---|---|
| Ames Research Center<br>Moffett Field, California 94035 | |
| | 13. Type of Report and Period Covered |
| 12. Sponsoring Agency Name and Address | Technical Memorandum |
| National Aeronautics and Space Administration<br>Washington, D. C. 20546 | 14. Sponsoring Agency Code |

15. Supplementary Notes

16. Abstract

A semiclassical model of the inelastic collision between a vibrationally excited anharmonic oscillator and a structureless atom is used to predict the variation of thermally averaged V-T rate coefficients with temperature and initial-state quantum number. Multiple oscillator states are included in a numerical solution for collinear encounters. The results are compared with CO-He experimental values for both ground and excited initial states using several simplified forms of the interaction potential. The numerical model is also used as a basis for evaluating several less complete but analytic models. Two computationally simple analytic approximations are found that successfully reproduce the numerical rate coefficients for a wide range of molecular properties and collision partners. Their limitations are also identified. Finally, the relative rates of multiple-quantum transitions from excited states are evaluated for several molecular types.

| 17. Key Words (Suggested by Author(s)) | 18. Distribution Statement |
|---|---|
| Vibrational energy transfer<br>Anharmonic oscillators<br>Rate coefficients<br>Multiple quantum transitions<br>Vibrationally inelastic collisions | Unlimited<br><br>STAR Category 72 |

| 19. Security Classif. (of this report) | 20. Security Classif. (of this page) | 21. No. of Pages | 22. Price* |
|---|---|---|---|
| Unclassified | Unclassified | 46 | $3.75 |

*For sale by the National Technical Information Service, Springfield, Virginia 22151

# Vibration-Translation Energy Transfer in Anharmonic Diatomic Molecules: II. The Vibrational Quantum-Number Dependence

Robert L. McKenzie

Ames Research Center, NASA, Moffett Field, California 94035

## I. INTRODUCTION

Modern applications of vibrational energy transfer frequently deal with processes that depend on the details of excitation for specific vibrational states. Infrared gas lasers are a primary example.[1] Of the several mechanisms influencing the population of a particular vibrational state, the collisional conversion of vibrational energy to translation can be an important aspect. For example, the probability of vibration-translation (V-T) energy transfer is well-known to increase as the quantum number of the initial state increases. Thus, even in situations where the V-T process may be insignificant to the kinetics of lower vibrational levels, it can dominate the flow of vibrational energy from upper levels and, in some cases, act as the primary path for vibrational energy loss from the system. The quantum-number dependence of V-T rates must therefore be considered in the analysis of most nonequilibrium processes where excess vibrational excitation has been produced. Unfortunately, very little quantitative information defining the V-T rate dependence on quantum number for even the simplest diatomic molecules is presently available from either experiment or theory. Experimental ground-state excitation rates have been obtained from measurements behind shock waves[2] or in fluorescence experiments[3] for many years but the difficulty of obtaining experimental V-T rates for molecules in well-defined excited vibrational states is indicated by the sparsity of attempts. Numerous experimenters have recently measured the rates of vibration-vibration (V-V) energy exchange between pairs of oscillators in excited states[4,5] because the fast V-V transfer can easily be made a dominant mechanism; but to date, only one comprehensive set of upper level V-T

rate measurements has been reported.[4] Even then, while the experiment was cleverly designed and carefully analyzed, the conditions were complex and the measurements required substantial correction to compensate for extraneous modes of energy transfer. Theoretical studies addressed to the analysis of initially excited oscillators have been similarly sparse. The usual theoretical interest has centered on harmonic oscillators initially in the ground state.[6] Simple analytic versions of these theories have frequently been applied in kinetic models to oscillators in excited states but their suitability in that application has not been validated.

The purpose of this study is to extend the present analytical situation by calculating the vibrational quantum-number dependence of V-T rate coefficients using a sufficiently complete collision model, which is not constrained to first-order approximations of the oscillator motion or its interactions. However, the approach to be taken is still limited by pragmatic considerations. Accurate V-T rate coefficient calculations by any theoretical model are obviated by uncertainties in the shape and magnitude of the interaction forces between colliding pairs for all but a few simple cases. Thus, we can only examine the qualitative features that are not masked by interaction potential uncertainties. Furthermore, even an extended collision model must retain some approximations, particularly regarding the collision geometry, if it is to remain computationally practical in the prediction of thermally averaged rate coefficients. Hence, a complete quantum-mechanical description of vibrationally inelastic encounters is avoided, although such descriptions have been formulated and solved with all degrees of completeness.[7-12] Instead, attention is confined here to a semiclassical treatment that accurately reproduces all

of the main characteristics of vibrational energy transfer to initially excited oscillators but may be further reduced to yield closed-form analytic solutions. The analytic solutions are of primary interest here because of their practical importance in the numerically cumbersome analysis of macroscopic nonequilibrium processes in which rate information for several modes of energy transfer must be economically provided.[1] The complete semiclassical model, requiring numerical solution, is applied both to an examination of the qualitative nature of upper state transitions and as a basis for evaluating the accuracy of the analytical solutions.

In the sections to follow, the features of the collision model that appear most important to the dynamics of a vibrationally excited oscillator are first discussed; followed by a description of several approximations, each of which retains one or more of the features considered. Approximate values of the interaction potential parameters and their range of uncertainty are then estimated by comparing the predicted ground-state rate coefficient with a comprehensive set of experimental values. Collisions of CO with He are chosen as the example because of the abundant data available. The implied potential parameters are then used to compare the numerical model with the experimental excited-state rate coefficients and with the analytic predictions. Finally, the effects of multiple-quantum transitions from excited states on a vibrational relaxation process are considered both for molecules like CO where the effect is secondary and for molecules like the halogens where the effect can be dominant.

## II. THE COLLISION MODEL

### A. Features influencing the excited state collision dynamics

As the quantum number of the initial oscillator state is increased, several aspects influencing the oscillator dynamics and its interactions with the incident particle gain increasing importance. For example, the wavefunctions describing vibrationally excited eigenstates become more extended in the oscillator coordinate. Consequently, when the oscillator is distorted by a collision, the wavefunction overlap is greater not only with adjacent eigenstates but with more remote states as well. This feature is reflected by the increased magnitude of the matrix elements dynamically coupling the eigenstates which, in turn, accounts for the greater probability of V-T energy transfer through both single- and multiple-quantum transitions. Furthermore, the increased coupling of nonadjacent states during the collision can affect the final occupation of states adjacent to the initial state and thereby influence the rate of single-quantum transitions. Thus, a calculation of the oscillator dynamics from an excited initial state must include multiple-state interactions at collision energies where they are normally unimportant for oscillators in the ground state.

The degree with which multiple-quantum transitions influence the oscillator dynamics during a collision depend, in part, on the form of the interaction potential. A common practice, often used to simplify the analysis of ground-state oscillators, is to consider the oscillator motion to be small compared to the range of interaction and linearize the interaction potential in the oscillator coordinate. In a harmonic

oscillator, this treatment has the effect of equalizing all of the diagonal matrix elements and forbidding multiple-quantum transitions. The occupation of nonadjacent oscillator states is then possible only through a sequence of single-quantum steps during the collision. Nonlinear interaction terms remove these restrictions and modify final state occupations in two related ways. First, all of the nonadjacent states are directly coupled, thereby increasing their accessibility. Second, the diagonal matrix elements are no longer equal, leading to additional phase distortions in the quantum-mechanical oscillator motion that modify the probability of transition. The additional phase shifts depend on the product of the difference between diagonal matrix elements and the strength of the interaction. They appear explicitly in a semiclassical impact parameter treatment described by Bates[13] and applied to anharmonic oscillators by Mies.[14] The formulation is reviewed in a subsequent section of this paper.

All of the foregoing effects are amplified when oscillator anharmonicity is included. Nonadjacent states become coupled even for linearized interactions and the larger difference between the diagonal matrix elements creates phase distortions that can become a significant fraction of the unperturbed oscillator period. Mies[14] has shown the influence on transition probability predictions to be large even for oscillators initially in the ground state. A second, and in some cases greater, effect of anharmonicity is its influence on the variation of eigenenergies with quantum number. Since transition probabilities and the related rate coefficients are well-known to depend on the amount of energy transferred, a lowest-order effect of oscillator anharmonicity may be demonstrated by

simply inserting anharmonic oscillator eigenenergies into a harmonic oscillator theory such as that given by Schwartz et al.[15] The results deviate substantially from the simple Landau-Teller relation for the rate coefficients given by

$$k_{m,m-1}(T) = mk_{1,0}(T) \tag{1}$$

where $k_{m,m-1}(T)$ denotes the rate coefficient for transitions from state m to m-1 and is a function of the kinetic temperature T. However, the simple ad hoc insertion of anharmonic eigenenergies into a harmonic oscillator model is not always a sufficient means of accounting for anharmonicity. The influence of anharmonicity on the interaction matrix elements, which in turn effects both the magnitude and phase of the oscillator motion, is often so great that an anharmonic oscillator model must be used from the start. Fortunately, oscillator anharmonicity and nonlinear interaction potentials present only a slight increase in computational difficulty, particularly if a Morse oscillator and an exponential form of the interaction are adopted. The necessary matrix elements are then conveniently expressed in closed algebraic form[9,14,16] just as they are for harmonic oscillators.

Finally, an oscillator potential creating anharmonicity also admits to the existence of continuum states. We shall neglect their contribution to the energy transfer process, however, since they are energetically inaccessible by a large margin for the combinations of collision energies and initial states to be considered here. Although no evaluation has been made of their effects, the occupation of continuum states is presumed

to be as small as the nearby bound states, and no bound states near the continuum were found to influence the dynamics of any states at the quantum levels of interest.

B. The semiclassical numerical model

To obtain V-T rate coefficients, we calculate the associated transition probabilities including oscillator anharmonicity and nonlinear interactions by treating the oscillator quantum-mechanically but calculating the collision trajectory classically. The trajectory is further constrained to collinear encounters. The unperturbed molecular wavefunctions are those of a quantized Morse oscillator and the interaction potential is composed of exponentially repulsive and, if desired, attractive terms. Formulation of the numerical model has been described in detail previously[16] but, in brief, an arbitrary multitude of coupled Morse eigenstates are included in a time-dependent numerical solution of the Schrödinger equation. Convergence is ensured by including a sufficient number of states above and below those of interest. The classical trajectory is coupled to the oscillator motion in a rigorous manner (within the semiclassical framework) guided by Ehrenfest's theorem. In effect, the classical path is influenced by the oscillator compression and recoil during the encounter. This feature successfully extends the semiclassical method to encounters where the average size of the oscillator is severely perturbed during the collision (e.g., when a light oscillator nucleus is struck by a heavy collision partner, as in $H_2$-He or CO-Ar collisions). The predicted transition probabilities have been shown[16] to reproduce the results from an equivalent collinear quantum-mechanical

calculation[9] over a wide range of conditions. We find, however, that although the semiclassical method is conceptually simpler and more easily reduced to an analytic formula, numerical solutions of the complete semiclassical model appear to be no more economical than exact quantum-mechanical solutions obtained using modern algorithms optimized for the roblem.[8,9] One of the penalties of using a semiclassical approximation is that total energy is not conserved, but the effects of that omission are easily and accurately compensated for by interpreting the relative collision energy or velocity as an average of the known initial and final values. A far more severe limitation of the semiclassical theory is its incomplete treatment of the interaction when the oscillator is very heteronuclear[16] (e.g., the hydrogen halides). Such cases are avoided here and have presented numerical difficulty in exact treatments.[9]

The implications introduced by a restriction to collinear encounters are not as well understood but the restriction is necessary if the quantum-number dependence of thermally averaged rate coefficients is ever to be obtained in a reasonable computing time. Clearly, a more realistic approach would include a three-dimensional collision geometry in which simultaneous rotational transitions are coupled with the vibrational motion. Considerable activity along these lines is currently evident[7-12,17,18] but the large number of rotational states that become accessible at collision energies sufficient to cause vibrational transitions would make our objective impractical for all but a few special molecules, like $H_2$. On the other hand, as long as the rotational eigenenergies of the undisturbed molecule are well-described by a rigid-rotor model (suggesting that the rotational and vibrational motion are separ-

able), the disparity between a collinear and a three-dimensional theory is not expected to be very sensitive to the initial vibrational quantum number. By normalizing the collinear predictions according to the ratio $k_{m,m-1}/mk_{1,0}$ and avoiding the prediction of absolute rate coefficients, much of the absolute error associated with the collinear restriction will hopefully be nullified. Such a ratio also absorbs the lowest-order quantum-number dependence suggested by Eq. (1).

## C. Thermally averaged rate coefficients from a collinear semiclassical model

With the possible exception of molecular beam analyses, the applications of an inelastic collision model usually require results in the form of a thermally averaged rate coefficient. A general formulation of the averaging integral is well-known but here the restriction to collinear trajectories and the use of a semiclassical approximation require some special consideration. In general, the rate coefficient for a kinetic temperature $T$ may be written in terms of the energy parameter $\epsilon_m = E_m/kT$ and an energy-dependent cross-section $\sigma_{m,n}(E_m)$, where $n$ denotes the final quantum state and $E_m$ is the relative kinetic energy before a collision with an undisturbed oscillator in a pure eigenstate $m$. The rate coefficient is then[19]

$$k_{mn}(T) = \overline{C} \int_0^\infty \sigma_{mn}(E_m) \epsilon_m e^{-\epsilon_m} d\epsilon_m \ , \tag{2}$$

where the average thermal speed is $\overline{C} = (8kT/\pi\mu)^{1/2}$ and $\mu$ is the reduced

collision mass. A further requirement for the collision model is that it conform to the detailed balance relations. Originating with the reciprocity theorem, the requirements of detailed balance propagate through three levels of microscopic detail, giving the general physical relations for spinless nondegenerate collision partners as

$$P_{mn}(E_m) = P_{nm}(E_n) \ , \tag{3a}$$

$$E_m\sigma_{mn}(E_m) = E_n\sigma_{nm}(E_n) \ , \tag{3b}$$

$$k_{mn}(T)e^{-\hbar\omega_m/kT} = k_{nm}(T)e^{-\hbar\omega_n/kT} \ , \tag{3c}$$

where $P_{mn}$ is the transition probability from state m to n and $\hbar\omega_m$ is the oscillator energy of state m.

The collinear collision geometry produces semiclassical transition probabilities that behave according to Eq. (3a) but the restriction to a zero impact parameter leaves the cross-section required by Eq. (2) undefined. One common solution is to adopt an effective hard-sphere cross-section $\sigma_o$ and compute the inelastic cross-section according to

$$\sigma_{mn}(E_m) = \sigma_o P_{mn}(E_m) \tag{4a}$$

and

$$\sigma_{nm}(E_n) = \sigma_o' P_{nm}(E_n) \ . \tag{4b}$$

Equation (3b) requires that

$$\sigma_o' = [1 + \hbar(\omega_n - \omega_m)/E_n]\sigma_o \ ,$$

thus suggesting that the "hard-sphere" size must depend on the collision energy and transition in question! This contradictory result is a consequence of the collinear approximation but the error is negligible when $|\hbar(\omega_n - \omega_m)|/E_n \ll 1$. In circumstances where the ratio approaches unity, the transition probability is typically so small that the integral in Eq. (2) is unaffected.

Equation (2) must be further modified to compensate for the lack of energy conservation inherent in the semiclassical approximation. This discrepancy is easily and accurately corrected by interpreting the semiclassical relative collision energy $\overline{E}$ or speed $\overline{u}$ as an average of the initial and final values. Reference 16 demonstrates that while the correction can be large, the method of averaging has no apparent effect on the outcome for vibrationally inelastic collisions at all energies from threshold up to the limits of practical interest. For convenience, we use an arithmetic energy average. Denoting the total energy as $E_T$, the semiclassical approximation is brought into close agreement with an equivalent quantum-mechanical calculation by the interpretation

$$\overline{E} = E_T - \hbar(\omega_m + \omega_n)/2 \ . \tag{5}$$

The combination of Eqs. (2), (4), and (5) then gives the thermal averaging prescription for a collinear semiclassical collision model as

$$k_{mn}(T) = \sigma_o \overline{C}\, e^{\hbar\omega_{mn}/2kT} \int_0^\infty P_{mn}(\overline{E}) \left( \epsilon + \left| \frac{\hbar\omega_{mn}}{2kT} \right| \right) e^{-\epsilon} d\epsilon \ , \tag{6}$$

where $\epsilon = \overline{E}/kT$ and $\omega_{mn} = \omega_m - \omega_n$. To make the satisfaction of Eq. (3c) by Eq. (6) more obvious, the lower integration limit in Eq. (6) has

been set to zero even though the independent variable transformation from $\epsilon_m$ to $\epsilon$ via Eq. (5) produces a limit of $\pm|\hbar\omega_{mn}/2kT|$, depending on the sign of $\omega_{mn}$. The negative limit may clearly be reset to zero but, even when the limit is positive, the probability threshold is nearly twice the limit, so that again setting it to zero has no effect on the integral.

## III. ANALYTIC APPROXIMATIONS

Of the many analytic approaches appearing in the literature (see Ref. 6 for a partial summary), three that stand out in their application for estimating the V-T rate coefficient variations with quantum number are (a) the semiempirical formulas for Morse oscillators of Keck and Carrier,[21] (b) the perturbation treatment of Morse oscillators developed by Mies,[14] and (c) the exact solution to a linearly forced harmonic oscillator obtained by Kerner.[22] Each approach retains one or more of the aspects of special interest to this application. They share the common feature that all incorporate collinear collision geometry and are all based on an exponentially repulsive interaction potential (later referred to as potential I) of the form

$$V_I(y) = Ae^{-y/L} , \tag{7}$$

where the coordinates are defined in Fig. 1 and transformed according to $y = \bar{x} - \gamma r$. The mass ratio $\gamma = m_c/(m_b + m_c)$ locates the mass center of the molecule and $L$ is an adjustable range parameter.

A. The Keck-Carrier formula for anharmonic oscillators

The formula obtained by Keck and Carrier[21] comes from an adaptation of the distorted-wave harmonic oscillator theory of Schwartz et al.[15] for a Morse oscillator. It includes an empirical fit to the numerical solution of an integral equation for the "adiabaticity factor" and provides a particularly simple formula for estimating single-quantum transition rates from an arbitrary initial state. Keck and Carrier[21] made no claim for the suitability of their formula in applications beyond a demonstration of the role of vibrational nonequilibrium in a dissociating gas; but the formula was subsequently applied by Bray[23] in a pioneering and detailed calculation of a vibrational relaxation process for anharmonic oscillators, apparently because of its simplicity and for lack of a better estimate. For similar reasons, the Keck-Carrier formula has since gained widespread use in the detailed analysis of upper state kinetics in lasers.[1] Its consideration here is motivated primarily by the number of kinetic models that incorporate it. The Keck-Carrier formula can be written in a form similar to Eq. (1) as[23]

$$k_{m,m-1}(T) = m\left(\frac{1-\chi_e}{1-m\chi_e}\right)\frac{F_m}{F_1}\,k_{1,0}(T)\ , \tag{8}$$

where $F$ is obtained from the empirical formula

$$F = \frac{1}{2}\left(3 - e^{4\pi\eta/3}\right)e^{4\pi\eta/3} \tag{9}$$

in which

$$\eta = -\omega_{m,m-1}L(\mu/2kT)^{\frac{1}{2}}\ . \tag{10}$$

The transition frequency $\omega_{m,m-1} = \omega_m - \omega_{m-1}$ is computed for a Morse oscillator from

$$\omega_m = \omega_e[(m+\tfrac{1}{2}) - \chi_e(m+\tfrac{1}{2})^2] \tag{11}$$

where $\omega_e$ is the fundamental oscillator frequency and $\chi_e$ is the anharmonic correction.

B. The Mies perturbation solution for anharmonic oscillators

The closest approximation to the numerical model used here is a semiclassical first-order perturbation treatment developed by Mies.[14b] It properly includes the effects of anharmonicity but, by the nature of first-order methods, it neglects the influence of states other than the designated initial and final states. Furthermore, to obtain an analytical solution the classical path must be computed independently from the motion of the oscillator. The theory is therefore applicable only to single-quantum transitions in which the transition probabilities are small compared to unity. The independent classical path further restricts its application to nearly homonuclear oscillators such as CO (and of course, all homonuclear molecules) colliding with atomic particles of lighter mass than either of the molecular nuclei.[16] The appearance of a probability maximum signals the failure of the theory.[16] In spite of these shortcomings, we shall see that Mies' solution still provides a more useful approximation of the numerical predictions than the other analytic formulas investigated. A convenient form of Mies' result for the transition probability from state m to n, where $n = m \pm 1$, can be written[14b,16]

$$P_{mn}(\bar{E}) = \left[\frac{V_{mn}}{V_{mm}} \frac{2\pi g\mu L\bar{u}}{\hbar \sinh(\pi g)} \Phi(-g,\lambda)\right]^2 , \qquad (12)$$

where $\bar{E}$ is the relative collision energy in a mass-centered reference frame and $\bar{u} = (2\bar{E}/\mu)^{\frac{1}{2}}$ is the corresponding speed. The other parameters are $g = L\omega_{mn}/\bar{u}$ and $\lambda = \mu L\bar{u}(V_{nn} - V_{mm})/\hbar V_{mm}$. The series function $\Phi(-g,\lambda)$ and the matrix elements $V_{mn}$ are defined in Appendix A. Note that equal diagonal matrix elements $V_{mm} = V_{nn}$ lead to $\Phi(-g,0) = 1$, reducing Eq. (7) to the equivalent formula for a harmonic oscillator with a linearized interaction.[14b]

As with the numerical model, Eq. (12) produces energy-dependent transition probabilities while a temperature-dependent rate coefficient is desired. No analytic solution of the integral Eq. (6) with $P_{mn}(\bar{E})$ given by Eq. (12) is apparent but a reasonably accurate technique (labeled "The Method of Steepest Descent") for obtaining an analytic approximation[6] is based on the well-defined maximum contained in the integrand of Eq. (6). The value of $\epsilon$ at which the maximum occurs is determined primarily by the exponential arguments.[6] The remaining function is slowly varying over the range of the integrand and may be evaluated at the single value $\epsilon_p$ locating the peak. The exponential argument is then expanded to second order about the peak and the term integrated analytically. In this application, the notation is simplified with the substitutions $\epsilon_{mn} \equiv \hbar\omega_{mn}/2kT$ and $\eta = -\omega_{mn}L(\mu/2kT)^{\frac{1}{2}}$. The exponential nature of Eq. (12) is also simplified by noting that in the energy range where the perturbation analysis is applicable, the transition period $t_p = 2\pi/\omega_{mn}$ is typically less than the effective collision period $t_c = 2L/\bar{u}$. Thus, $\pi g = t_c/t_p > 1$ and $\sinh(\pi g) \approx \frac{1}{2}e^{\pi g}$. Equations

(6) and (12) are then combined to give

$$k_{mn}(T) = \sigma_o \bar{C} \left[\frac{V_{mn}}{V_{mm}} 4\pi \frac{\eta^2}{\epsilon_{mn}}\right]^2 e^{\epsilon_{mn}} \int_0^\infty (\bar{\epsilon} + |\epsilon_{mn}|)\, \phi^2\, e^{-\bar{\epsilon}+2\pi\eta\bar{\epsilon}^{-1/2}}\, d\bar{\epsilon} \ . \qquad (13)$$

The integrand peak is located at

$$\epsilon_p = [\mu(\pi\omega_{mn}L)^2/2kT]^{1/3} \ . \qquad (14)$$

Using the procedure described, the approximate solution to Eq. (13) becomes

$$k_{mn}(T) = 16(3\pi^3)^{-1/2}\sigma_o \bar{C} \left(\frac{V_{mn}}{V_{mm}} \frac{\epsilon_p^3}{\epsilon_{mn}}\right)^2 \epsilon_p^{1/2}(\epsilon_p + |\epsilon_{mn}|)\, \phi^2(-g_p, \lambda_p)$$
$$\times e^{-3\epsilon_p + \epsilon_{mn}} \left\{1 + \mathrm{erf}\left[(3\epsilon_p/4)^{1/2}\right]\right\} \qquad (15)$$

where $g_p = \epsilon_p/\pi$ and $\lambda_p = \epsilon_p^2(V_{mm} - V_{nn})/\pi\epsilon_{mn}V_{mm}$ . The error function in Eq. (15) is close to unity for most cases. Equation (15) has log k $\alpha$ $T^{-1/3}$ as expected and satisfies Eq. (3c). The temperature at which a given collision speed is coincident with the peak of the integrand in Eq. (13) defines the most effective speed at that temperature; this temperature will also be useful and can be identified from Eq. (14) as

$$T_p = \mu\bar{u}^3/2\pi k|\omega_{mn}|L \ . \qquad (16)$$

Comparisons of the approximate integration of Eq. (13) with exact numerical integrations show that the approximate method is most accurate at low temperatures. The first-order perturbation formula, Eq. (12), is most accurate at low energies, thus further contributing to the accuracy of Eq. (15) at low temperatures.

## C. The Kerner solution for linearly forced harmonic oscillators

The final analytic formula to be considered is an exact solution obtained by Kerner[22] for a harmonic oscillator that undergoes a forcing function linear in the oscillator coordinate. That condition may be satisfied in situations where $r/L \ll 1$ in Eq. (7). The potential may then be linearized according to

$$V(\bar{x},r) = Ae^{-\bar{x}/L}(1-\gamma r/L) \ . \tag{17}$$

Kerner's solution was applied by Treanor[24] in a semiclassical collinear approximation using Eq. (17). Within the framework of the collision model, the resulting formula exactly calculates the probability of transitions between arbitrary states with the interaction of all states included. Thus, it can be applied at high collision energies where the interactions of more than two states influence the oscillator dynamics. In spite of the approximate nature of the harmonic oscillator model, wherein direct multiple-quantum transitions and the unbalanced coupling of higher and lower states caused by anharmonicity are excluded, the Kerner solution remains useful because it offers the only analytic means of estimating transition probabilities at high energies. Examples will be shown where multiple-quantum transitions and oscillator anharmonicity are not dominant, allowing accurate prediction by the Kerner solution.

Kerner[22] and Treanor[24] write the probability for transitions between two arbitrary states $m$ and $n$ as

$$P_{mn}(\bar{E}) = m!n!\, e^{-E_o} E_o^{m+n}\left\{\sum_{j=0}^{J}\left[(-E_o)^j (m-j)!\, j!\, (n-j)!\right]^{-1}\right\}^2 \ , \tag{18}$$

where $J$ is the lesser of the quantum numbers $m$ and $n$. The parameter $E_o$ is the energy absorbed by a classical harmonic oscillator divided by one quantum of vibrational energy. For a collinear collision and the interaction of Eq. (17), Rapp[25] obtains

$$E_o = 2(2\pi\omega L\gamma\mu)^2 \, e^{-2\pi\omega L/\bar{u}}/\hbar\omega\mu_o \, . \tag{19}$$

In Eq. (19), $\mu_o$ is the reduced mass of the oscillator and $\omega$ is the oscillator frequency. The accuracy of the model, when applied to highly excited oscillators, is substantially improved if the effective oscillator frequency is corrected for anharmonicity for each initial state $m$ according to $\omega = \omega_e(1 - 2\chi_e m)$. Without the correction, the excited-state rate coefficients would simply behave according to the Landau-Teller relation, Eq. (1), at low temperatures where the effective values of $E_o$ are all less than unity and give $k_{m,m-1}/mk_{1,0} < 1$ for large $E_o$. An inconvenience of the Kerner formula is its incompatibility with the approximate integration method of Eq. (6) for obtaining a rate coefficient. A simplified version of Eq. (18), assuming $E_o << 1$, permits an approximate analytical solution. However, the calculations are then restricted to a thermal range where multiple-quantum effects are insignificant and the theory loses its advantages over perturbation solutions. In the comparisons to follow, we have therefore resorted to a numerical integration of Eq. (6) when the Kerner solution is applied.

## IV. COMPARISONS WITH CO-He EXPERIMENTS

In this section, the ability of the theoretical model to reproduce experimental rate coefficients is tested. Unlike past comparisons of vibrational rate coefficients with theory, we now have access to at least one set of experimental values for excited initial states.[4] To test the consistency of the theory and experiment for all vibrational states, however, the effective interaction range $L$ and the hard-sphere cross-section $\sigma_o$ are determined from the abundant collection of measurements dominated by transitions between the ground state and first vibrational state. The interaction parameters required to match the ground-state experiments are then applied in comparisons with the excited-state rate measurements.

### A. Effective interaction parameters

The computational convenience gained from the simplified interaction potential I, Eq. (7), justifies its use, but as a consequence of its simplified form, the predicted rate coefficients cannot be expected to reproduce the experiments at all kinetic temperatures. Transitions induced in an oscillator depend to a large extent on the potential gradient near the distance of closest approach; while in a collinear collision, the distance of closest approach is determined mainly by the coordinate where the potential magnitude equals the initial kinetic energy of the collision. The magnitude of a purely repulsive potential, such as Eq. (7), and that of a more realistic potential with an attractive well may be the same at the closest approach distance but have a significantly dif-

ferent gradient. Consequently, where collisions are averaged over a range of energies, the predicted variation of rate coefficients with kinetic temperature will be different for the two potentials. By matching theory and experiment in several thermal ranges, and by using more than one potential form, an indication of the degree of uncertainty in rate coefficients attributable to potential errors can be obtained. For that purpose, we consider a second potential given by

$$V_{II}(y) = D\, e^{(y_o-y)/L} - 2D\, e^{(y_o-y)/2L} . \qquad (20)$$

Potential II is a Morse-type interaction with an attractive well of depth $-D$ at coordinate $y_o$. As with Eq. (7), the exponential form allows matrix elements to be calculated analytically.

Predictions by the numerical anharmonic oscillator model with the oscillator initially in the first eigenstate $m = 1$ are compared with experiment in Fig. 2. When potential I, Eq. (7), is used, the rate coefficients are independent of the magnitude $A$, so that only the range $L$ requires specification. Similarly, the predictions using potential II are independent of $y_o$ but require both $L$ and $D$ to be specified. The value $D/k = 100°K$ is representative of well depths inferred from viscosity measurements.[26] The two potential gradients are different by about 20% at closest approach for the typical conditions considered. Figure 2 demonstrates the expected results. No unique set of potential parameters reproduces the experiments over the complete thermal range but the more realistic potential II comes the closest. The required values of $L$ fall between 0.02 nm and 0.03 nm, depending on the thermal range considered.

As an interesting aside, note that the low temperature departure of the experimental rate from a variation proportional to $T^{-1/3}$ is also followed by the theory using simple repulsive potentials. As Shin[27] points out, these low temperature departures do not necessarily depend on weak attractive forces normally omitted from the interaction potential; they even occur with a repulsive potential when the thermal averaging integration is done accurately for low collision energies. We know, however, that real interaction potentials usually contain an attractive component and it will augment this low temperature behavior.

B. Comparisons with excited-state rate measurements

Normalized rate coefficients, predicted for initially excited CO at $T = 300°K$, are compared in Fig. 3 with the room temperature measurements of Hancock and Smith.[4] The parameter $k_{m,m-1}/mk_{1,0}$ is much less sensitive to interaction uncertainties than the absolute rate coefficients and varies in a simple, nearly linear manner with initial-state quantum number $m$. The nearly linear quantum-number dependence, increasing with $m$ at room temperature, is predicted for all of the interaction potentials examined and is believed to be an accurate description of the real behavior. As Fig. 3 shows, the experimental excited-state values compare favorably in magnitude with the predictions, but their trend is inconsistent with a linear extrapolation to $m = 1$. A highly nonlinear extrapolation is contrary to any prediction of the collision model at any temperature. Although the collision model contains many simplifications awaiting refinement, the behavior implied by the experimental

rates appears also to require further verification and extension. In the interim, the theoretical predictions of excited state rates seem to be qualitatively reasonable and self-consistent in spite of their quantitative uncertainty. Unfortunately, their verification by experiment remains inconclusive.

## V. AN EVALUATION OF THE ANALYTIC APPROXIMATIONS

The computational expense of the numerical model makes it impractical as a general means of estimating excited-state rate coefficients. Instead, it is used in this section as a basis for evaluating the more convenient but less complete analytic formulas. The predicted rate coefficient variations with quantum number for several models are illustrated in Fig. 4 for two extreme temperatures. The differences in the various models depend strongly on the kinetic temperature but they all predict a simple monotonic change with quantum number. The analytic approximations are therefore more clearly evaluated by choosing the highest initial quantum number of practical interest and then comparing the predictions for a range of temperatures. In the case of CO, Lordi et al.[1(e)] have shown that energy transfer from vibrational levels as high as the twentieth can influence the net energy balance in an electrically excited CO laser system. Choosing $m = 20$, the single-quantum rate coefficients predicted by all of the collision models are compared in Fig. 5. The independent parameter $(\hbar\omega_e/kT)^{\frac{1}{2}}$ was chosen so that predictions by the Keck formula, Eq. (8), appear as a nearly straight line. A comparison of the rates from the numerical model using potentials I and II shows the moderate sensitivity of $k_{m,m-1}/mk_{1,0}$ to the form of the potential

for one potential range L at all temperatures. Not shown is the great sensitivity of the magnitude of $k_{m,m-1}/mk_{1,0}$ to other potential ranges at any temperature. Note, however, that the qualitative nature of the predictions are undisturbed by the form of the potential and therefore considered realistic. As expected, the Mies solution, Eq. (15), accurately reproduces the numerical results at low temperatures but fails at higher temperatures where multiple-state interactions begin to affect the single-quantum transitions. The departure is signaled when transition probabilities approaching unity influence the thermal averaging integral, Eq. (6). Since CO is not very anharmonic, the Kerner harmonic oscillator model, Eq. (18), frequency-corrected for anharmonicity at $m = 20$, works well over the entire thermal range. Note that the anharmonic correction must be included, however, as all predictions are significantly above the result stated by Eq. (1) for a single-frequency harmonic oscillator. Finally, Fig. 5 shows that the Keck formula, Eq. (8), is too crude an approximation for large initial quantum numbers.

The degree of oscillator distortion caused by the collision of a light helium atom with a CO molecule has an insignificant effect on the classical trajectory. This fact is made evident by the small difference at low temperatures between the numerical model where the effect is included and the Mies solution where it is neglected. An example in which the coupling is larger is illustrated in Fig. 6 for CO($m = 20$)-Ar collisions. In this situation, none of the analytic models do well at low temperatures because the effects of oscillator distortion on the classical path modifies the transition probabilities even near threshold. The small corrections are then greatly amplified by the thermal averaging integral at low temperatures.

The small anharmonicity of CO($\chi_e = 0.0062$) has influenced the preceding examples mainly by altering the energy spacing between excited eigenstates. Anharmonicity also modifies the absolute magnitude of the rate coefficients but that effect is not apparent in the ratio $k_{m,m-1}/mk_{1,0}$. An example in which the anharmonicity is large is illustrated in Fig. 7 for $H_2$(m = 10)-He($\chi_e = 0.0268$). In this case, the frequency-corrected harmonic oscillator model is inaccurate at all temperatures. The large spacing between eigenenergies in $H_2$ suppresses the onset of multistate interactions at high temperatures, making the Mies solution an accurate reproduction of the numerical results over the entire thermal range. The difference in mass between the He and H nuclei produces only moderate coupling between the compressed oscillator and the classical path.[16]

As the preceding comparisons indicate, one cannot generally choose a single analytic model for estimating excited-state rate coefficients that is applicable to all collision pairs. The situations where a model should not be used are easier to identify. Clearly, the Keck formula, Eq. (8), is too approximate in all of the examples. The Kerner harmonic oscillator solution, Eq. (18), with anharmonicity-corrected frequencies is reasonably accurate unless the anharmonicity is large. The Mies anharmonic oscillator solution, Eq. (15), is a poor approximation when multiple-state interactions become important. Finally, no analytic model based on the semiclassical approximation will be realistic when the oscillator dynamics have a significant influence on the classical path of the incident particle. This restriction limits all of the models considered to collision pairs in which the mass of the incident particle is not

significantly greater than the mass of the impacted nucleus and to oscillators that are not extremely heteronuclear.

## VI. MULTIPLE-QUANTUM TRANSITIONS

In the preceding section, only transitions to an adjacent state have been examined. Here, we investigate the relative importance of multiple-quantum transitions, particularly for oscillators in highly excited states. The probabilities of multiple-quantum transitions are compared in Fig. 8 both for CO(m)-He collisions in which the oscillator is initially in an excited state and in states near the ground state. The collision speeds contributing most to the thermally averaged rate coefficient at a selected temperature are indicated by the effective temperature $T_p$. In the thermal range considered, multiple-quantum transitions to the ground-state are always improbable compared to single-quantum transitions from the first vibrational level, but the situation is clearly different when the oscillator is initially in the twentieth quantum state. However, thermally averaging the transition probabilities in Fig. 8 reduces the apparent importance of multiple-quantum transitions in a relaxation process. Figure 9 illustrates the resulting rate coefficients for two potential ranges, using potential I and values of $\sigma_o$ obtained from the experimental match in Fig. 2 at $T = 1000°K$. The amplified uncertainty caused by the interaction potential and its influence on the implied value of $\sigma_o$ is most obvious but the qualitative features are again consistent for both potential ranges. For oscillators like CO, multiple-quantum transitions provide a significant path for energy transfer only at very high temperatures, according to these predictions.

A temperature marking the onset of competitive multiple-quantum transitions is the characteristic vibrational temperature of the oscillator, here defined as $\theta_v = \hbar\omega_e/k$ (for CO, $\theta_v = 3122°K$). An oscillator in which multiple-quantum transitions will dominate the relaxation process can then be identified if $\theta_v$ is small. One extreme example is $Br_2$ for which $\theta_v = 465°K$. Since the anharmonicity is also small in $Br_2$ ($\chi_e = 0.0033$), the Kerner harmonic oscillator model has been used to obtain the $Br_2$-He rate coefficients displayed in Fig. 10. Two- and three-quantum transitions from the tenth vibrational level are shown to be significant even at room temperature and the temperature dependence of the single-quantum rate ($m \to n = 10 \to 9$) is inverted by multiple-state interactions. The high probability of multiple-quantum transitions in this case contributes to the extremely fast and thermally insensitive relaxation rates measured in the halogens and destroys the concept of a single "relaxation time"[19] that is independent of the nonequilibrium state of the process for molecules of this type.

## VII. CONCLUDING REMARKS

We have relied on a collinear semiclassical model for vibrationally inelastic collisions entirely for pragmatic reasons. The collinear geometry affords an economically reasonable means of estimating V-T rate coefficients for excited molecules and the semiclassical approximation is easily reduced to practical analytic solutions. While these simplifications clearly obviate the quantitative accuracy of the calculations, no serious omission is apparent that would modify their qualitative nature, even in the presence of uncertain interaction potentials.

Unfortunately, an attempt to confirm the predicted features through experimental comparison was inconclusive. However, the experimental conditions that would test the model most severely can at least be identified. For example, the choice of collision partner has a large influence on the rate coefficient sensitivity to initial quantum number. Note the large deviations of $k_{m,m-1}/mk_{1,0}$ from unity in Fig. 6 for CO-Ar compared to those for CO-He in Fig. 5. Furthermore, the increased oscillator distortion caused by heavy atom impact requires a more complete description of the interaction than needed for light atoms. From another viewpoint, the lesser sensitivity of some features of the prediction to uncertainties can guide the choice of experimental variables to be emphasized. In particular, an apparently universal feature of the V-T excited-state rate predictions is their monotonic low-order variation with quantum number. Once this feature is confirmed, the experimental emphasis can be shifted to the less predictable variations with kinetic temperature. Finally, a comparison of the estimates using various potential parameters suggest that a self-consistent set of experimental rates for both high and low initial quantum numbers contains much more information defining the interaction potential than ground-state rates alone.

Comparisons of the analytic and numerical rate coefficients graphically delineate the suitable range of application for each analytic model. However, the utility of an analytic approximation can also depend on the physical properties of the application. For example, the Kerner-Treanor harmonic oscillator model, with anharmonically corrected frequencies, predicts the ratio $k_{m,m-1}/mk_{1,0}$ with surprising accuracy for many molecules; but before the model can be economically applied, an

analytical solution to the thermal averaging integral, including Kerner's transition probability formula, awaits development. Even with that solution in hand, one must be concerned with the effect of anharmonicity for each molecule treated by the model. On the other hand, Mies' solution for anharmonic oscillators, Eq. (15), fails at high temperature. At those conditions, however, many nonequilibrium processes are insensitive to the V-T rates of excited states, either because the vibrational state population distribution is nearly Boltzmann or because the process is controlled by some separate energy transfer mechanism. At lower temperatures, the model accurately deals with a broader range of oscillators because anharmonicity is rigorously included. Collision partners for which the theory fails are poorly treated by all the analytic solutions based on a semiclassical approximation. Similarly, the frequently employed formula developed by Keck[8] is useful because of its simplicity but the additional computation required by the Mies solution is not prohibitive. The series function $\Phi(-g,\lambda)$ converges rapidly and the matrix elements may be computed in advance.

The calculations of multiple-quantum transition rates from excited states validate the assumption most often made in kinetic models of nonequilibrium processes: they can usually be neglected. As before, at very high temperatures where multiple-quantum transitions become competitive, a nonequilibrium process is usually not controlled by excited-state V-T rates while ground-state transitions are still dominated by single-quantum steps. Molecules with closely spaced vibrational energy levels, such as the halogens, are notable exceptions requiring a more careful analysis.

## APPENDIX A

The series function $\Phi(-g,\lambda)$ and the matrix element $V_{mn}$ for an anharmonic oscillator are given here in algebraic terms for use in Eqs. (12) and (15). A more complete description of their origin is given in Ref. 16. The series function is computed according to

$$\Phi(-g,\lambda) = \sum_{\ell=1}^{\infty} A_\ell \lambda^{\ell-1} , \tag{A1}$$

where $A_1 = 1$, $A_2 = -g$. The remaining coefficients are obtained by the recurrence formula

$$\ell(\ell-1)A_\ell = -2gA_{\ell-1} - A_{\ell-2} \tag{A2}$$

The matrix elements, defined by $V_{mn} = \langle n|e^{\gamma r/L}|m\rangle$, are most easily computed in terms of the parameters $\alpha = \gamma/aL$, $\beta = \chi_e^{-1}$, and $a = 2\pi\omega_e(2\mu_o\chi_e)^{\frac{1}{2}}$ where all variables are defined in the main text. The result is[9,14,16]

$$V_{mn} = \beta^\alpha \frac{N_m N_n}{a} \frac{\Gamma(\beta-n)}{m!} \sum_{\ell=0}^{n} \frac{(-1)^{\ell+n-m}}{\ell!(n-\ell)!} \frac{\Gamma(1+\alpha+n-\ell)\ \Gamma(\beta-\alpha-1-n)}{\Gamma(1+\alpha+n-m-\ell)\ \Gamma(\beta-2n+\ell)} . \tag{A3}$$

In Eq. (A3), $\Gamma(z)$ is the gamma function with argument $z$ and the normalization constants are

$$N_j = [a(\beta-1-2j)/\Gamma(\beta-j)]^{\frac{1}{2}} . \tag{A4}$$

REFERENCES

[1](a) R. E. Center and C. E. Caledonia, Appl. Optics 10, 1795 (1971); (b) J. W. Rich, J. Appl. Phys. 42, 2719 (1971); (c) R. L. McKenzie, Phys. Fluids 15, 2163 (1972); (d) R. J. Hall and A. C. Eckbreth, IEEE J. Quant. Elec. 10, 580 (1974); (e) J. A. Lordi, T. J. Falk, and J. W. Rich, AIAA paper no. 74-563, AIAA 7th Fluid and Plasma Dynamics Conference, Palo Alto, California, 1974.

[2]R. C. Milliken, J. Chem. Phys. 40, 2594 (1964).

[3](a) R. C. Milliken, J. Chem. Phys. 38, 2855 (1963) (b) D. J. Miller and R. C. Milliken, J. Chem. Phys. 53, 3384 (1970); (c) W. H. Green and J. K. Hancock, J. Chem. Phys. 59, 4326 (1973).

[4]G. Hancock and I. W. M. Smith, Appl. Optics 10, 1827 (1971).

[5](a) I. W. M. Smith and C. Wittig, J. Chem. Soc. (Trans. Faraday Soc. II) 69, 939 (1973); (b) H. T. Powell, J. Chem. Phys. 59, 4937 (1973); (c) R. M. Osgood, Jr., P. B. Sackett, and A. Javan, J. Chem. Phys. 60, 1464 (1974); (d) Y. Fushki and S. Tsuchiya, Japan. J. Appl. Phys. 13, 1043 (1974). Note: Many other similar papers have recently appeared, too numerous to catalog.

[6]D. Rapp and R. Kassal, Chem. Rev. 69, 61 (1969).

[7]E. Eastes and D. Secrest, J. Chem. Phys. 56, 640 (1972).

[8]D. Secrest and B. R. Johnson, J. Chem. Phys. 45, 4556 (1966).

[9]A. P. Clark and A. S. Dickinson, J. Phys. B: Atomic, Mol. Phys. 6, 164 (1973).

[10]H. Rabitz and G. Zarur, J. Chem. Phys. 61, 5076 (1974).

[11]P. McGuire, J. Chem. Phys. 62, 525 (1975).

[12]D. J. Kouri and C. A. Wells, J. Chem. Phys. 61, 2296 (1974).

[13]D. R. Bates, Quantum Theory. I. Elements (Academic, New York, 1961), p. 252.

[14](a) F. H. Mies, J. Chem. Phys. 40, 523 (1964); (b) ibid. 41, 903 (1964).

[15](a) R. N. Schwartz, Z. I. Slawsky, and K. F. Herzfeld, J. Chem. Phys. 20, 1591 (1952); (b) K. F. Herzfeld and T. A. Litovitz, Absorption and Dispersion of Ultrasonic Waves (Academic, New York, 1959).

[16]R. L. McKenzie, NASA TMX 62406 (Submitted to J. Chem. Phys., 1975).

[17]C. F. Hansen and W. E. Pearson, J. Chem. Phys. 53, 3557 (1970).

[18]J. D. Kelly and M. Wolfsberg, J. Chem. Phys. 53, 2967 (1970).

[19]W. G. Vincenti and C. H. Kruger, Jr., Introduction to Physical Gas Dynamics (Wiley, New York, 1965).

[20]L. D. Landau and E. M. Lifshitz, Quantum Mechanics (Pergamon, Oxford, 1958), p. 432.

[21]J. Keck and G. Carrier, J. Chem. Phys. 43, 2284 (1965).

[22]E. H. Kerner, Can. J. Phys. 36, 371 (1958).

[23]K. N. C. Bray, J. Phys. B. (Proc. Phys. Soc.) Ser. 2 1, 705 (1968).

[24]C. E. Treanor, J. Chem. Phys. 43, 532 (1965).

[25]D. Rapp, J. Chem. Phys. 32, 735 (1960).

[26]J. O. Hirschfelder, C. F. Curtiss, and R. W. Bird, Molecular Theory of Gases and Liquids (Wiley, New York, 1954), p. 1111.

[27](a) H. K. Shin, J. Chem. Phys. 55, 5233 (1971); (b) ibid. 57, 1363 (1972).

FIGURE CAPTIONS

FIG. 1. Collinear collision geometry.

FIG. 2. A comparison of experimental rate coefficients for CO(m = 1)-He transitions to the ground vibrational state with predictions from the numerical model[16] for anharmonic oscillators. The solid and long-short dash lines were computed using the repulsive interaction potential I, Eq. (7). The short dash line was computed using the Morse interaction potential II, Eq. (20). Hard-sphere collision cross-sections were chosen for each potential to match the experiment at T = 1000°K. Experimental values are from: ○ Ref. 2, ● Ref. 3a, Δ Ref. 3b, ◆ Ref. 3c.

FIG. 3. A comparison of experimental rate coefficients at T = 300°K for CO(m)-He transitions from vibrational states m to m - 1 with predictions from the numerical model using repulsive potential I, Eq. (7). The excited-state data are from Ref. 4 and have been normalized using the experimental $k_{1,0}$ value of Milliken[2,3] (Fig. 2).

FIG. 4. The CO(m)-He rate coefficient dependence on quantum number predicted by several collision models. The solid lines represent the anharmonic numerical model,[16] the long-short dash lines represent the Kerner harmonic oscillator solution,[22] Eq. (18), and the dashed lines are from the formula of Keck,[21] Eq. (8). The potential range L = 0.02 nm, was used in all cases.

FIG. 5. A comparison of excited-state rate coefficients for CO(m = 20)-He predicted by several collision models. The potential range was L = 0.02 nm in all cases.

FIG. 6. A comparison of excited-state rate coefficients for CO(m = 20)-Ar. Potential I, Eq. (7), was used with L = 0.02 nm in all cases.

FIG. 7. A comparison of excited-state rate coefficients for $H_2$(m = 10)-He. Potential I, Eq. (7), was used with L = 0.02 nm in all cases.

FIG. 8. Multiple-quantum transition probabilities for CO(m)-He collisions using the anharmonic numerical model with potential I and L = 0.02 nm. The effective temperature $T_p$ locates the most effective collision speed contributing to the thermally averaged rate coefficient at the temperature designated.

FIG. 9. Multiple-quantum rate coefficients for CO(m)-He. Potential I was used in the anharmonic numerical model. The hard-sphere cross-section values $\sigma_o$ for each potential range are those required to match the experimental rates in Fig. 2 at T = 1000°K.

FIG. 10. Multiple-quantum rate coefficients for $Br_2$(m)-He predicted using the Kerner harmonic oscillator solution, Eq. (18), with L = 0.02 nm.

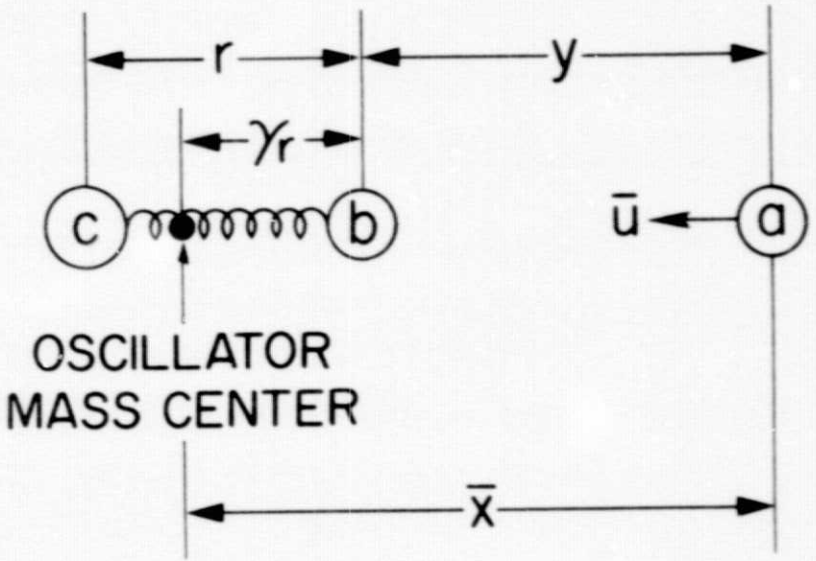


FIG. 1. Collinear collision geometry.

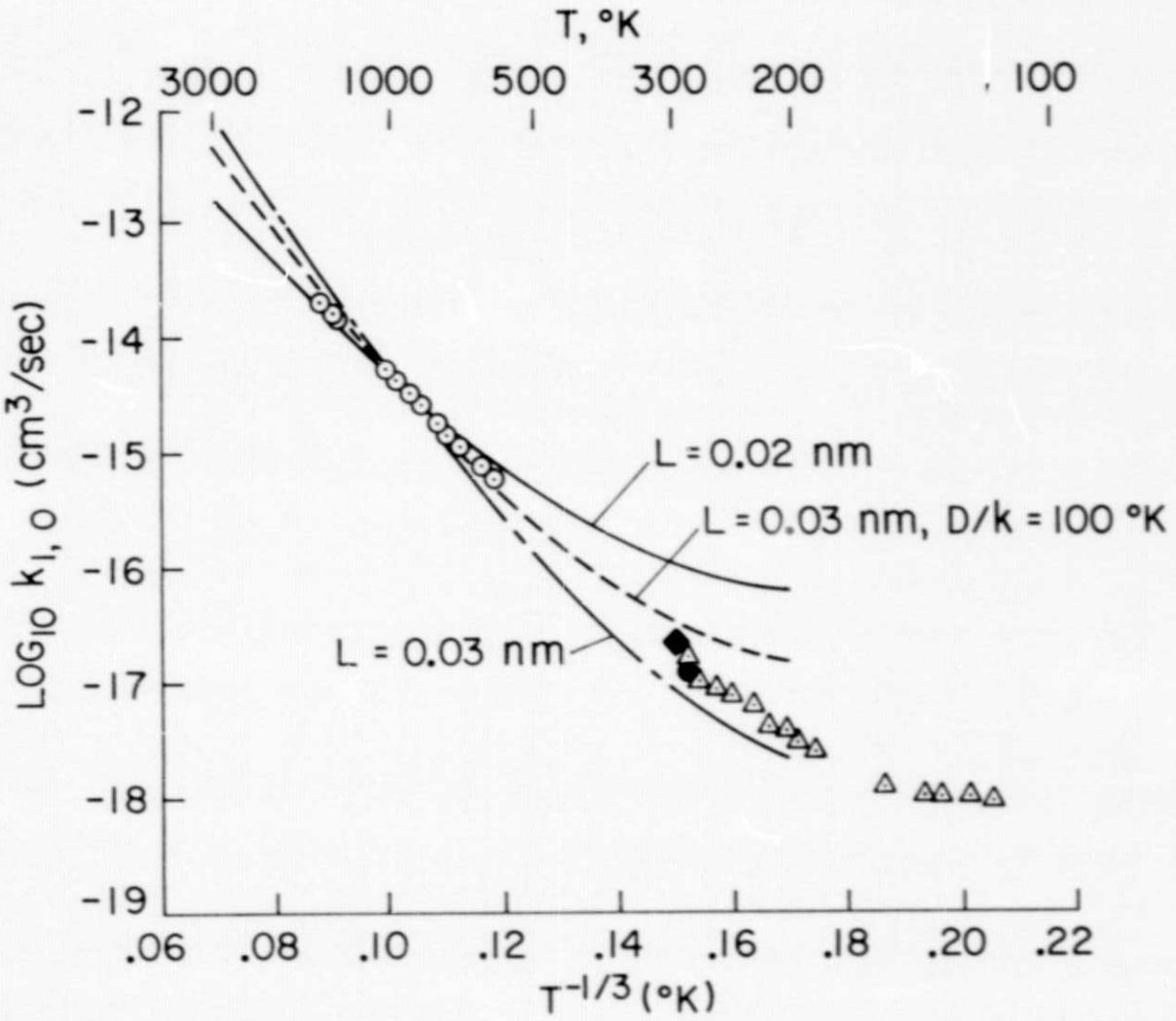


FIG. 2. A comparison of experimental rate coefficients for CO(m = 1)-He transitions to the ground vibrational state with predictions from the numerical model[16] for anharmonic oscillators. The solid and long-short dash lines were computed using the repulsive interaction potential I, Eq. (7). The short dash line was computed using the Morse interaction potential II, Eq. (20). Hard-sphere collision cross-sections were chosen for each potential to match the experiment at T = 1000°K. Experimental values are from: ○ Ref. 2, ● Ref. 3a, △ Ref. 3b, ◆ Ref. 3c.

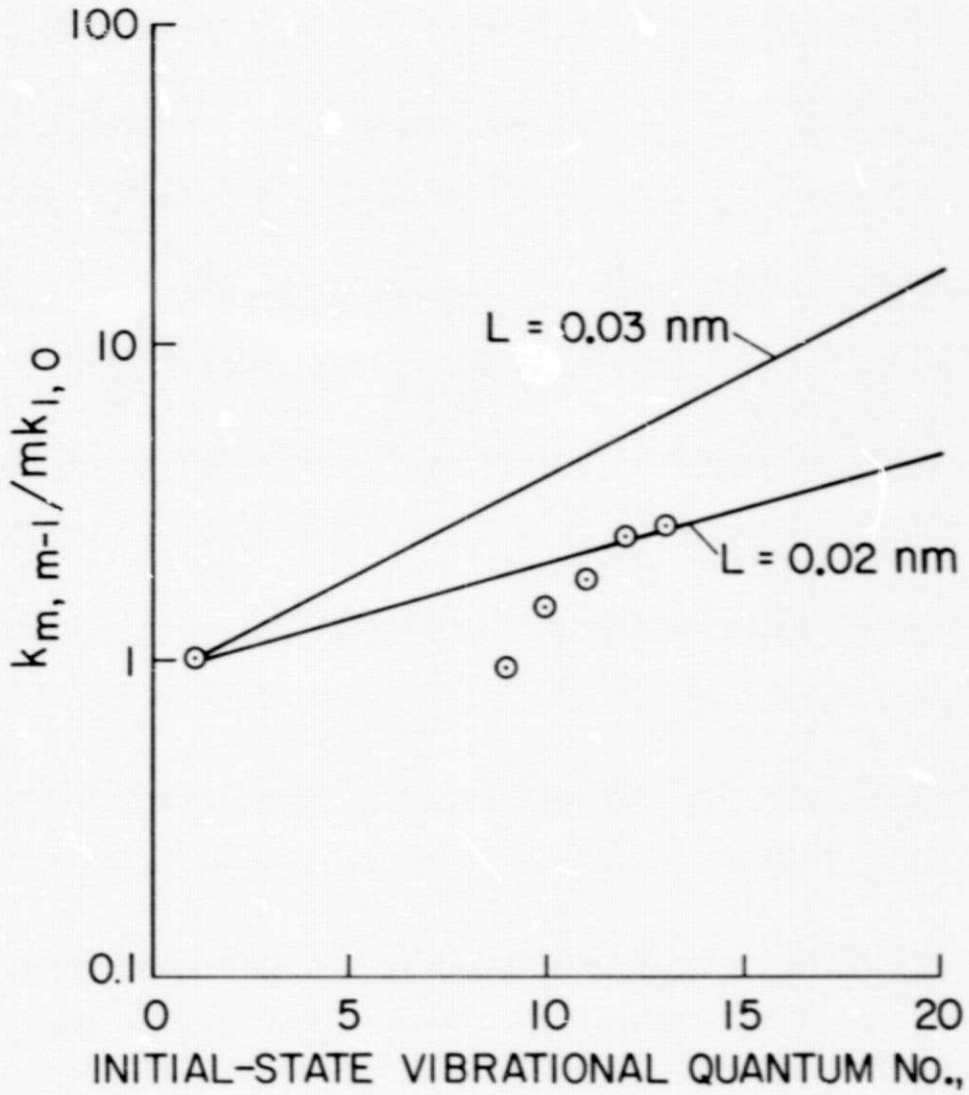


FIG. 3. A comparison of experimental rate coefficients at T = 300°K for CO(m)-He transitions from vibrational states m to m - 1 with predictions from the numerical model using repulsive potential I, Eq. (7). The excited-state data are from Ref. 4 and have been normalized using the experimental $k_{1,0}$ value of Milliken[2,3] (Fig. 2).

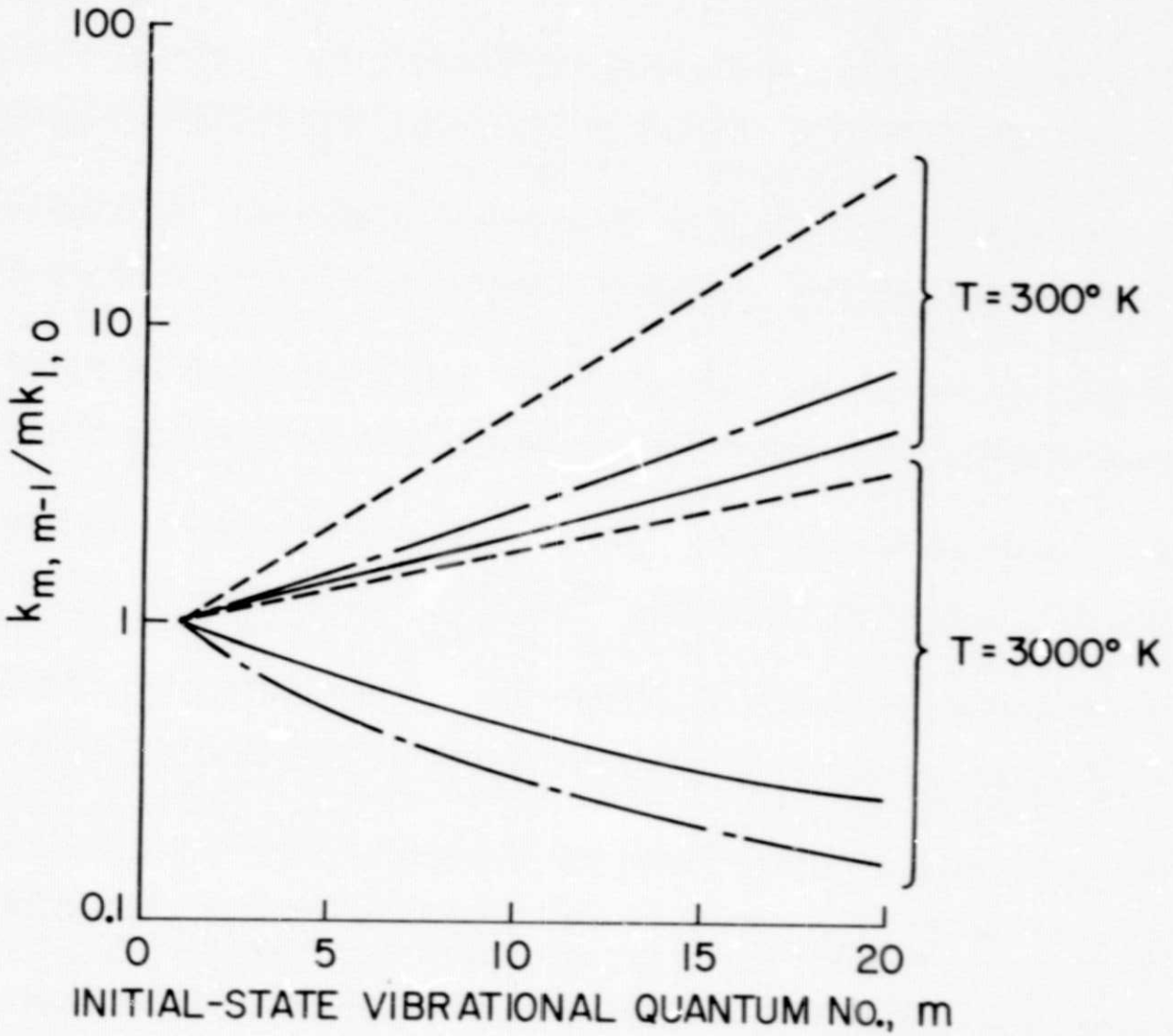


FIG. 4. The CO(m)-He rate coefficient dependence on quantum number predicted by several collision models. The solid lines represent the anharmonic numerical model,[16] the long-short dash lines represent the Kerner harmonic oscillator solution,[22] Eq. (18), and the dashed lines are from the formula of Keck,[21] Eq. (8). The potential range L = 0.02 nm, was used in all cases.

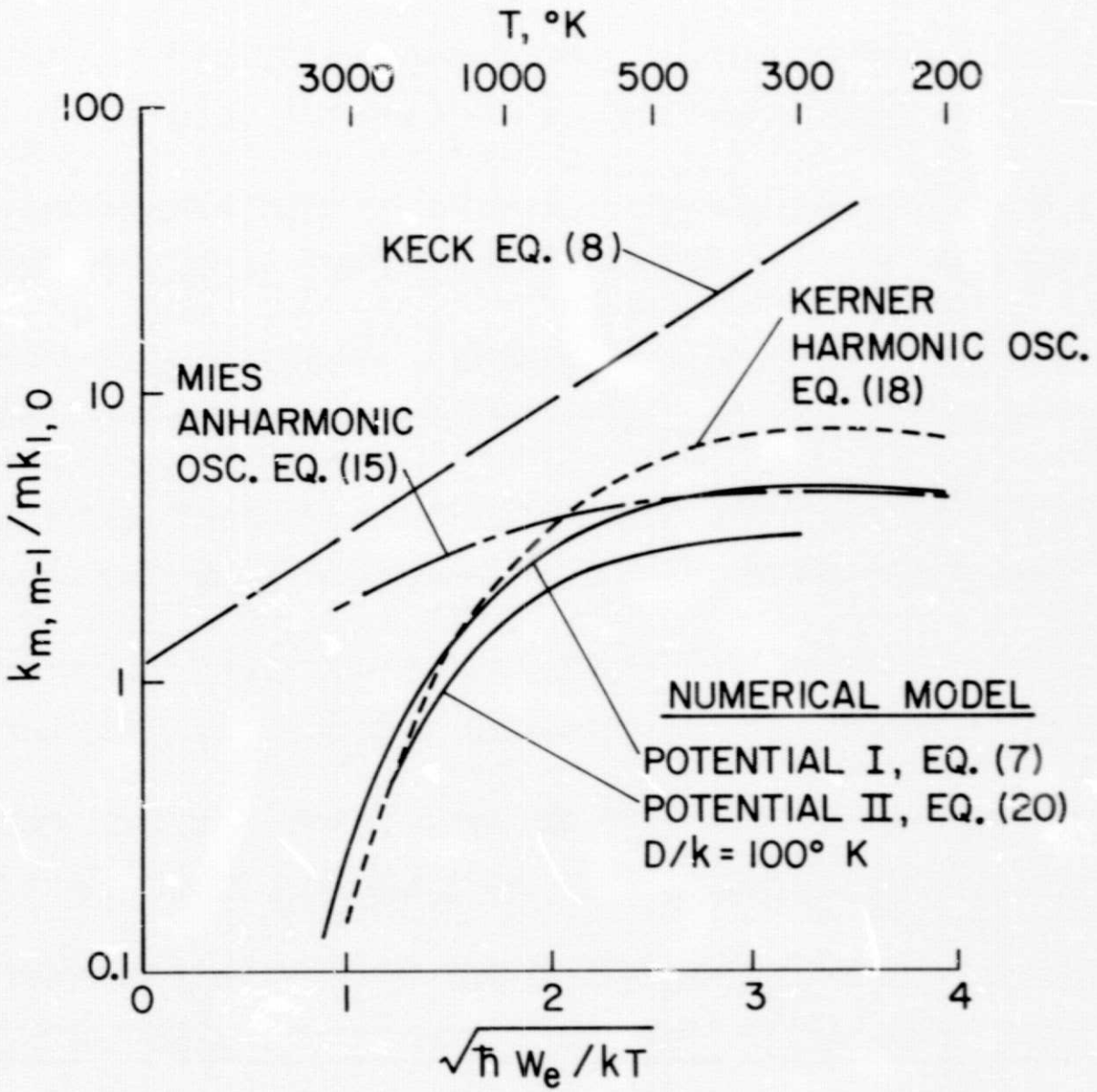


FIG. 5. A comparison of excited-state rate coefficients for CO(m = 20)-He predicted by several collision models. The potential range was L = 0.02 nm in all cases.

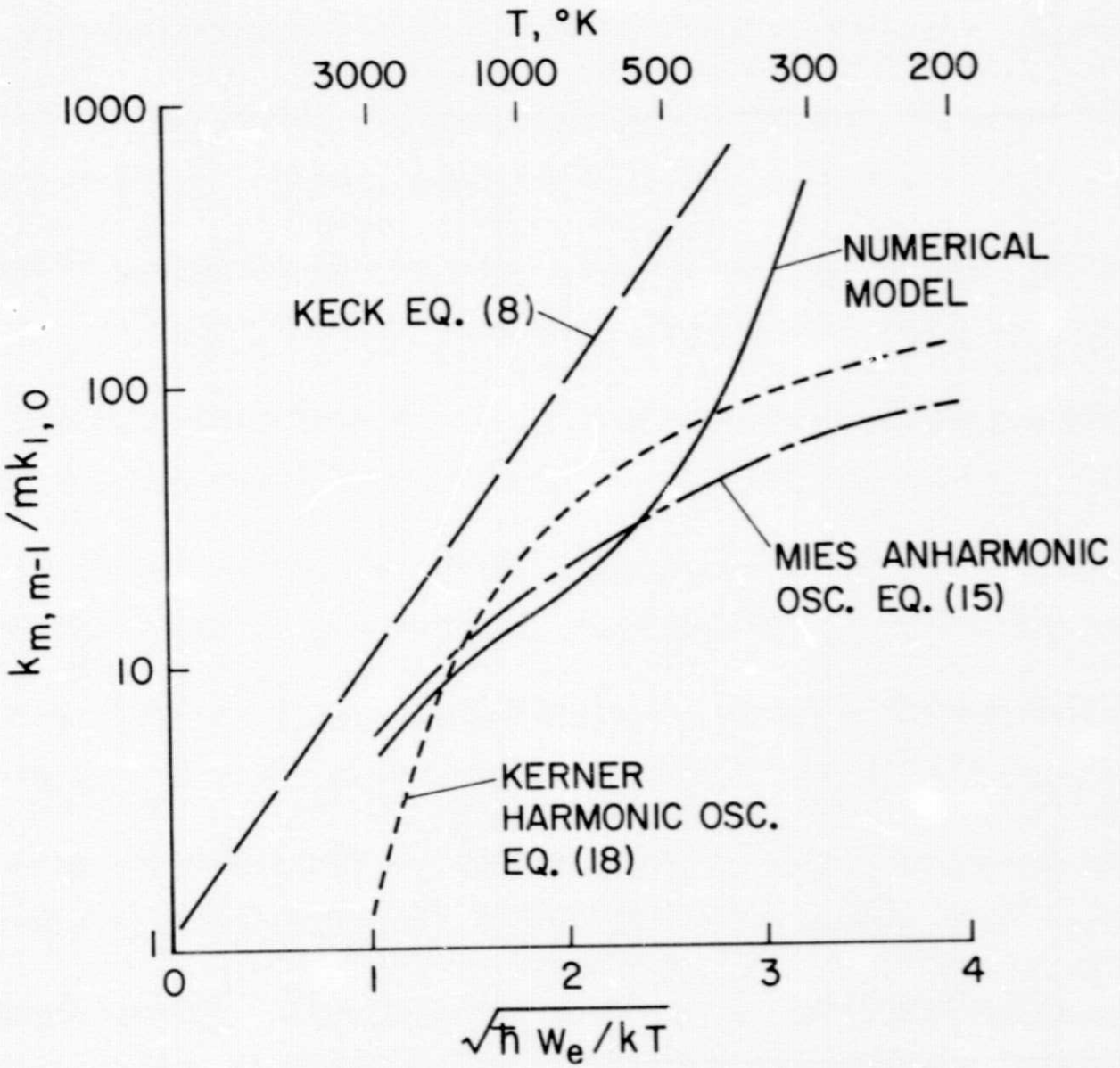


FIG. 6. A comparison of excited-state rate coefficients for CO(m = 20)-Ar. Potential I, Eq. (7), was used with L = 0.02 nm in all cases.

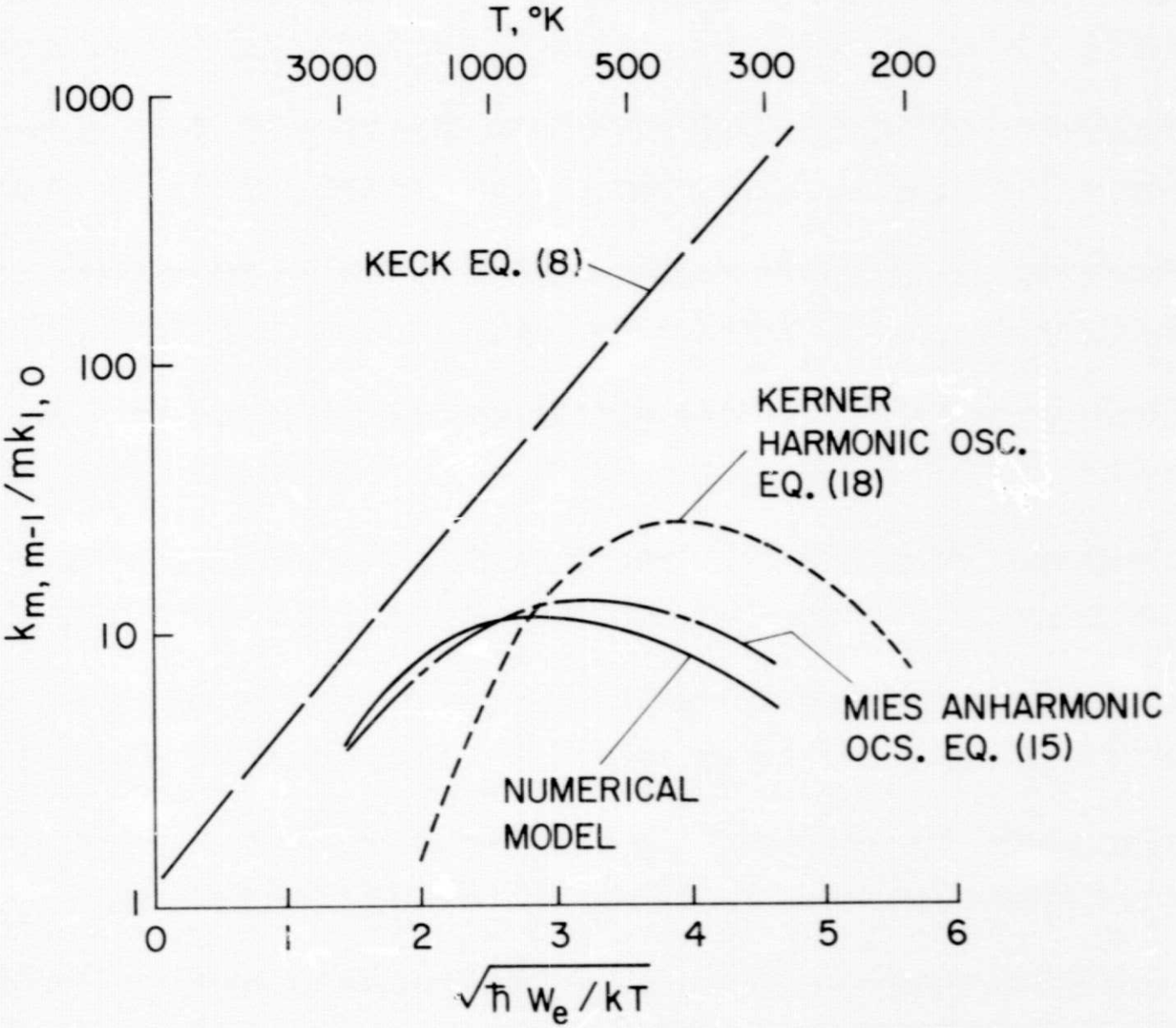


FIG. 7. A comparison of excited-state rate coefficients for $H_2(m = 10)$-He. Potential I, Eq. (7), was used with L = 0.02 nm in all cases.

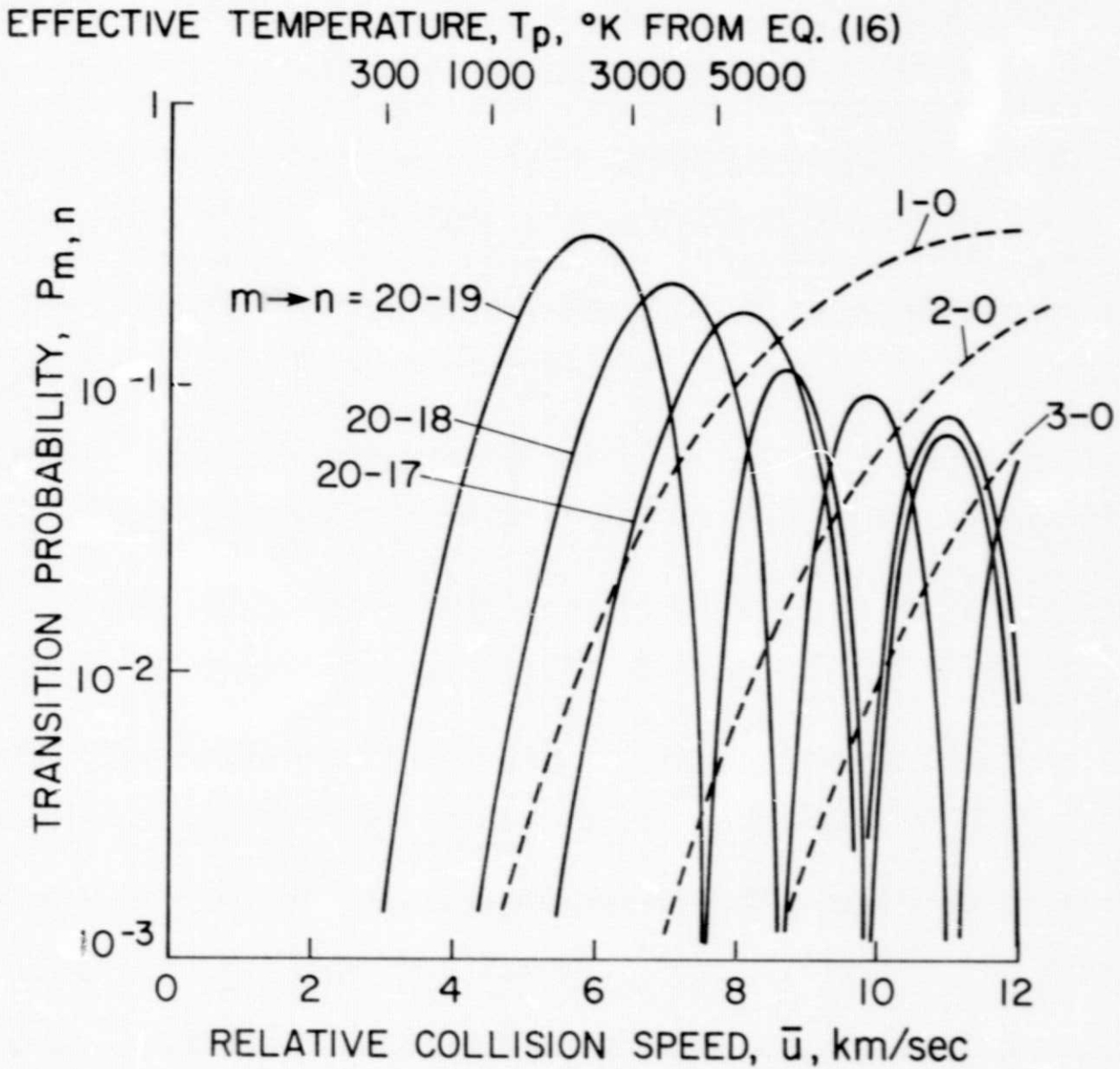


FIG. 8. Multiple-quantum transition probabilities for CO(m) - He collisions using the anharmonic numerical model with potential I and L = 0.02 nm. The effective temperature $T_p$ locates the most effective collision speed contributing to the thermally averaged rate coefficient at the temperature designated.

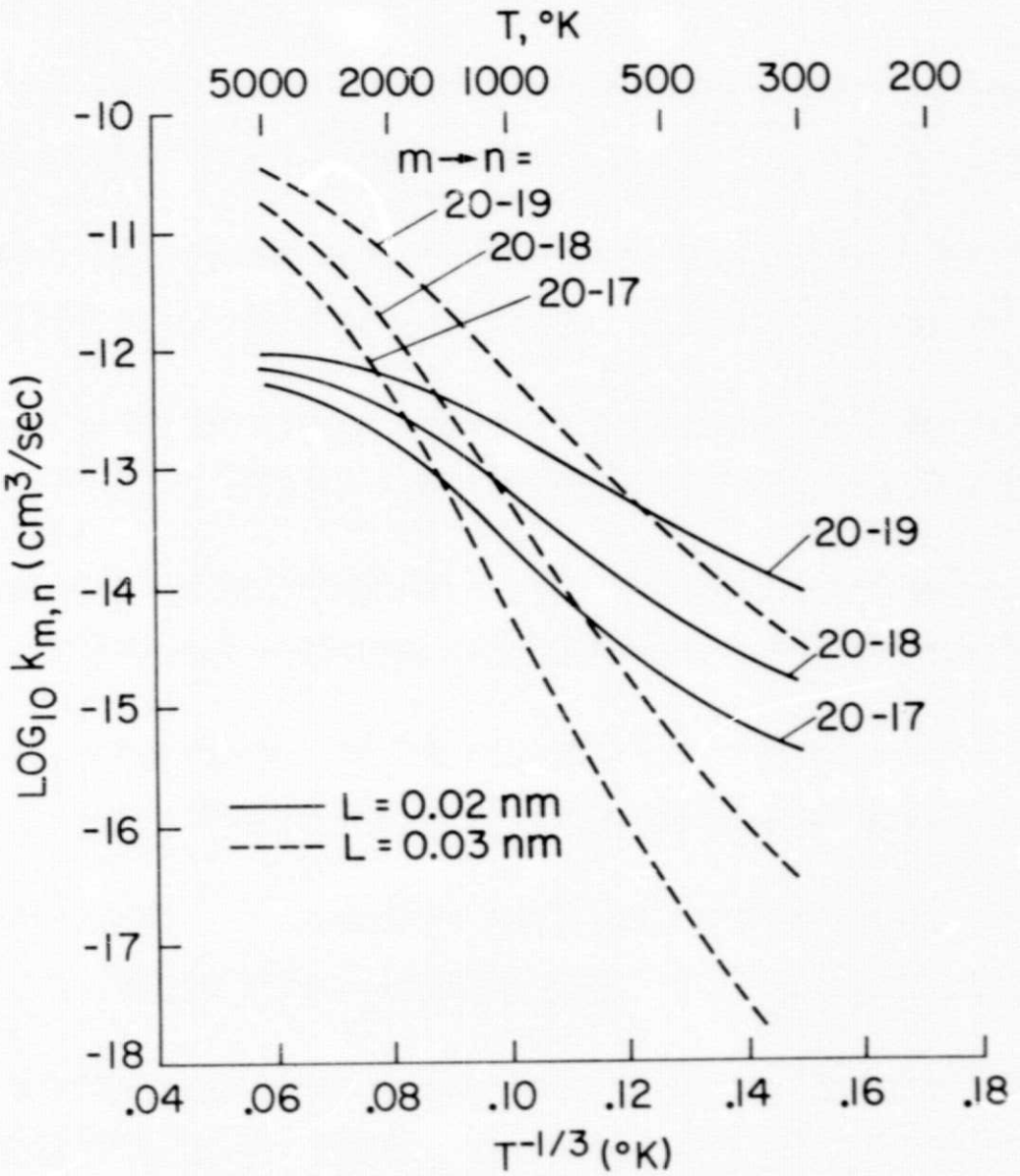


FIG. 9. Multiple-quantum rate coefficients for CO(m)-He. Potential I was used in the anharmonic numerical model. The hard-sphere cross-section values $\sigma_o$ for each potential range are those required to match the experimental rates in Fig. 2 at T = 1000°K.

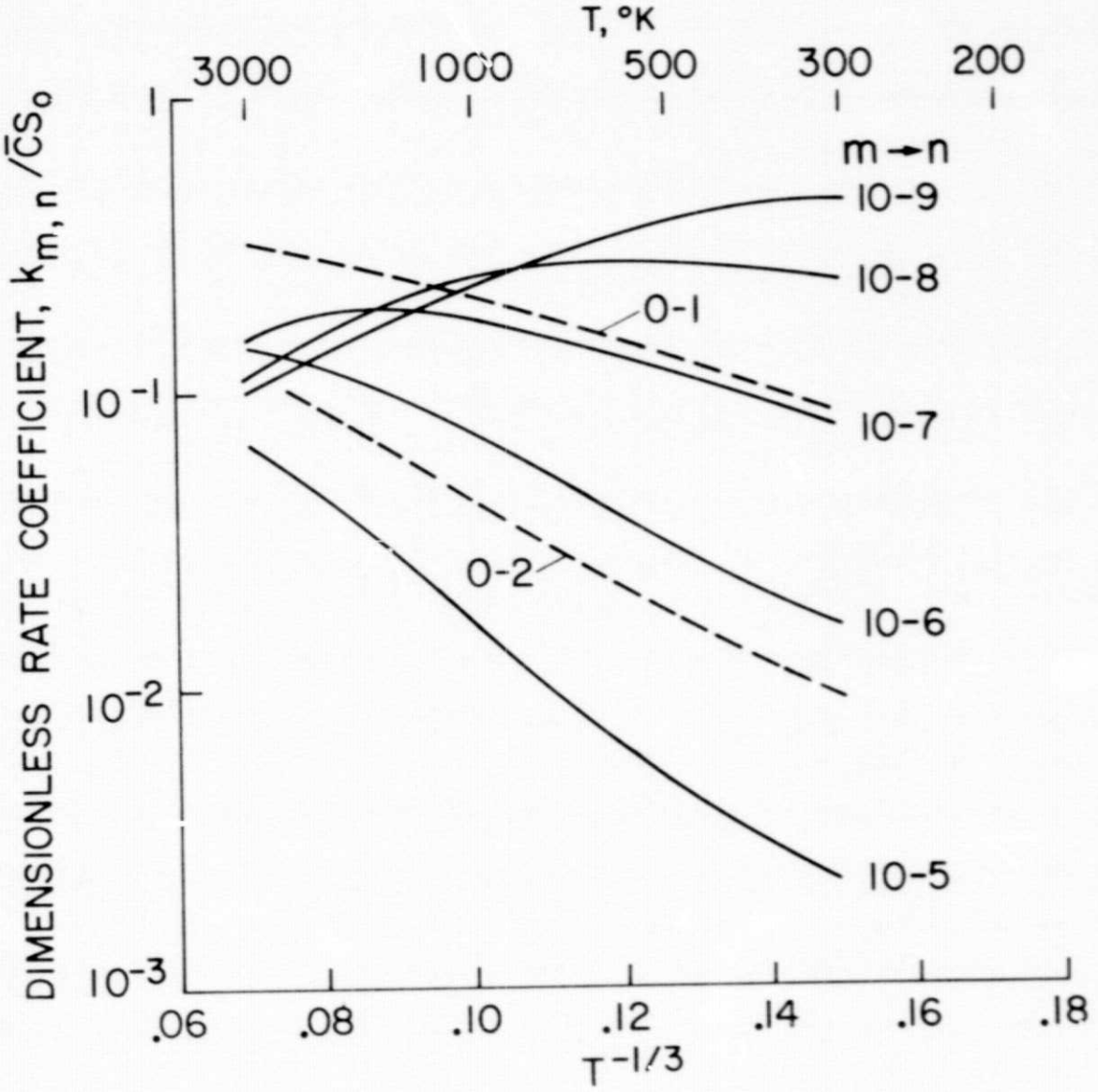


FIG. 10. Multiple-quantum rate coefficients for $Br_2(m)$-He predicted using the Kerner harmonic oscillator solution, Eq. (18), with L = 0.02 nm.